

Novel CHK1 inhibitor MU380 exhibits significant single-agent activity in TP53-mutated chronic lymphocytic leukemia cells

Miroslav Boudny,¹ Jana Zemanova,¹ Prashant Khirsariya,^{2,3} Marek Borsky,¹ Jan Verner,¹ Jana Cerna,¹ Alexandra Oltova,¹ Vaclav Seda,^{1,4} Marek Mraz,^{1,4} Josef Jaros,⁵ Zuzana Jaskova,¹ Michaela Spunarova,¹ Yvona Brychtova,¹ Karel Soucek,^{3,6,7} Stanislav Drapela,^{3,6,7} Marie Kasparkova,¹ Jiri Mayer,¹ Kamil Paruch,^{2,3} and Martin Trbusek¹

¹Department of Internal Medicine, Hematology and Oncology, University Hospital Brno and Faculty of Medicine, Masaryk University; ²Department of Chemistry, CZ Openscreen, Faculty of Science, Masaryk University; ³Center of Biomolecular and Cellular Engineering, International Clinical Research Center, St. Anne's University Hospital; ⁴Center of Molecular Medicine, Central European Institute of Technology, Masaryk University; ⁵Department of Histology and Embryology, Faculty of Medicine, Masaryk University; ⁶Department of Cytokinetics, Institute of Biophysics CAS, v.v.i. and ⁷Department of Experimental Biology, Faculty of Science, Masaryk University, Brno, Czech Republic

ABSTRACT

Introduction of small-molecule inhibitors of B-cell receptor signaling and BCL2 protein significantly improves therapeutic options in chronic lymphocytic leukemia. However, some patients suffer from adverse effects mandating treatment discontinuation, and cases with *TP53* defects more frequently experience early progression of the disease. Development of alternative therapeutic approaches is, therefore, of critical importance. Here we report details of the anti-chronic lymphocytic leukemia single-agent activity of MU380, our recently identified potent, selective, and metabolically robust inhibitor of checkpoint kinase 1. We also describe a newly developed enantioselective synthesis of MU380, which allows preparation of gram quantities of the substance. Checkpoint kinase 1 is a master regulator of replication operating primarily in intra-S and G₂/M cell cycle checkpoints. Initially tested in leukemia and lymphoma cell lines, MU380 significantly potentiated efficacy of gemcitabine, a clinically used inducer of replication stress. Moreover, MU380 manifested substantial single-agent activity in both *TP53*-wild type and *TP53*-mutated leukemia and lymphoma cell lines. In chronic lymphocytic leukemia-derived cell lines MEC-1, MEC-2 (both *TP53*-mut), and OSU-CLL (*TP53*-wt) the inhibitor impaired cell cycle progression and induced apoptosis. In primary clinical samples, MU380 used as a single-agent noticeably reduced the viability of unstimulated chronic lymphocytic leukemia cells as well as those induced to proliferate by anti-CD40/IL-4 stimuli. In both cases, effects were comparable in samples harboring p53 pathway dysfunction (*TP53* mutations or *ATM* mutations) and *TP53*-wt/*ATM*-wt cells. Lastly, MU380 also exhibited significant *in vivo* activity in a xenotransplant mouse model (immunodeficient strain NOD-*scid* IL2R γ^{null}) where it efficiently suppressed growth of subcutaneous tumors generated from MEC-1 cells.

Introduction

Significant progress has been achieved in the therapy of chronic lymphocytic leukemia (CLL) with the introduction of small-molecule inhibitors targeting the B-cell receptor (BCR) signaling^{1,2} and BCL2 protein.³ Drugs like ibrutinib, idelalisib or venetoclax are currently changing clinical practice in CLL treatment. The most extensive data are related to the BCR inhibitor ibrutinib, and besides many positive aspects revealed also that: (i) the drug possesses a specific toxicity profile enforcing treatment



Haematologica 2019
Volume 104(12):2443-2455

Correspondence:

MARTIN TRBUSEK
Trbusek.Martin@fnbrno.cz

KAMIL PARUCH
paruch@chemi.muni.cz

Received: July 31, 2018.

Accepted: April 5, 2019.

Pre-published: April 11, 2019.

doi:10.3324/haematol.2018.203430

Check the online version for the most updated information on this article, online supplements, and information on authorship & disclosures: www.haematologica.org/content/104/12/2443

©2019 Ferrata Storti Foundation

Material published in *Haematologica* is covered by copyright. All rights are reserved to the Ferrata Storti Foundation. Use of published material is allowed under the following terms and conditions:

<https://creativecommons.org/licenses/by-nc/4.0/legalcode>.

Copies of published material are allowed for personal or internal use. Sharing published material for non-commercial purposes is subject to the following conditions:

<https://creativecommons.org/licenses/by-nc/4.0/legalcode>, sect. 3. Reproducing and sharing published material for commercial purposes is not allowed without permission in writing from the publisher.



discontinuation in a proportion of patients;⁴ (ii) some patients progress during therapy to the stage of highly adverse diffuse large B-cell lymphoma (Richter transformation);⁵ and (iii) relapsed/refractory patients harboring 17p deletion (*TP53* defect) experience relatively short progression-free survival and overall survival after the single-agent ibrutinib treatment.^{6,7} Nevertheless, the clinical efficacy of ibrutinib is substantially better compared to chemoimmunotherapy, which has been found to be unsuitable for *TP53*-defective patients.⁸

Replication is a vital process for each cancer cell, and the proteins controlling its course represent interesting targets for anti-cancer therapy. The checkpoint kinase 1 (CHK1) supervises replication through the intra-S and G₂/M cell cycle checkpoints, where it stabilizes stalled replication forks after DNA damage and participates in DNA repair by homologous recombination process.^{9,10} CHK1 is an important member of the DNA damage response (DDR) pathway, which represents a fundamental anti-cancer barrier.¹¹ Central to DDR are two signaling cascades: ATR→CHK1 and ATM→CHK2→p53. While the latter is frequently mutated in tumors, the activity of *ATR* and *CHEK1* genes is essential for cell survival.^{12,13} In line with this, *CHEK1* was found to be an essential gene for 557 out of 558 cancer cell lines, according to the DepMap database (depmap.org) (*Online Supplementary Figure S1*).

Numerous structurally diverse CHK1 inhibitors have been developed as potentiating agents, i.e. for combination with chemotherapy. Nevertheless, some of them showed interesting pre-clinical single-agent activity against diverse cancer types, including breast and ovarian cancer,¹⁴ small-cell lung cancer,¹⁵ colorectal cancer,¹⁶ neuroblastoma,¹⁷ melanoma,¹⁸ MYC driven lymphoma,¹⁹ and leukemia.^{20,21} Currently, several CHK1 inhibitors are undergoing evaluation in clinical trials focusing on solid tumors and hematologic malignancies. In CLL, CHK1 inhibition represents a potentially attractive concept for the following reasons: (i) CHK1 is essential for normal B-cell development and lymphomagenesis;²² (ii) leukemia and lymphoma cells are particularly vulnerable to CHK1 depletion;²⁰ and (iii) CLL cells are sensitive to manipulation with the level of replication stress (RS), as shown in experiments inhibiting ATR, a CHK1 upstream kinase.²³

In our previous study,²⁴ we employed one of the most selective CHK1 inhibitors, SCH900776,²⁵ and showed that it significantly potentiates activity of fludarabine in *TP53*-mutated CLL cells, as well as in a CLL *TP53*-wt mouse model. Subsequently, we developed compound MU380, a non-trivial analog of SCH900776 which contains unusual N-trifluoromethylpyrazole moiety protecting the molecule from oxidative dealkylation and thus improving its metabolic stability.²⁶ With our current study, we present a robust enantioselective synthesis of MU380, and demonstrate its single-agent efficacy in lymphoid cancer cells. Significantly, to the best of our knowledge, we have for the first time demonstrated the potential for CHK1 inhibition to affect high-risk CLL cells with *TP53* defects.

Methods

CHK1 inhibitors

Compound SCH900776 (Merck; MK-8776) was prepared in-house using previously described procedure.²⁴ Compound MU380 was also prepared in-house using our newly developed

enantioselective synthesis (see Results section and *Online Supplementary Appendix*). These inhibitors were stored at room temperature as 10 mM stock solutions dissolved in DMSO.

Cell lines and primary chronic lymphocytic leukemia cells

Leukemia and lymphoma cell lines were obtained from the German Collection of Microorganisms and Cell Cultures (DSMZ) and cultured in accordance with DSMZ recommendations. *TP53* mutation status was verified by sequencing, and was in accordance with the International Agency for Research on Cancer database.²⁷ The origin of non-cancerous cell lines is provided in *Online Supplementary Appendix*. Primary CLL samples consisting of peripheral blood mononuclear cells (PBMNC) with >90% leukemic cells were obtained from patients treated at the Department of Internal Medicine, Hematology and Oncology of the University Hospital Brno. Written informed consent was signed by all patients, and the study was approved by the Ethics Committee of the University Hospital Brno (Project n. 15-33999A). After thawing, CLL cells were cultured in RPMI-1640 medium with 10% FBS and penicillin/streptomycin. Genetic characterization of the samples is described in *Online Supplementary Table S3*.

Pro-proliferative stimulation of chronic lymphocytic leukemia cells

Pro-proliferative stimulation of CLL cells was made using the anti-CD40 + IL-4 system developed by Patten *et al.*²⁸ and used by us previously.²⁴ Here we made the following modifications: the ratio of CLL cells to murine fibroblasts (irradiated by 50 Gy) was 20:1 and length of stimulation was ten days; fresh medium (half volume), and fresh mAb anti-CD40 and IL-4 (full doses of 200 ng/mL and 10 ng/mL, respectively) were added on days 3 and 7. On day 10, CLL cells were gently removed and cultured for an additional three hours (h) to allow residual fibroblasts to attach. For viability testing, CLL cells were transferred to 96-well plates and treated with MU380 or DMSO (mock control).

Transfection of chronic lymphocytic leukemia cells

The cells were transfected by electroporation using Neon Transfection System (Thermo Fisher Scientific) according to the manufacturer's instructions. Detailed information is provided in the *Online Supplementary Appendix*.

Cell viability assays, immunoblotting, real-time polymerase chain reaction, analyses of cell cycle, apoptosis and mitotic cells

Detailed information on all methodologies is provided in the *Online Supplementary Appendix*.

Xenograft experiments

Experiments were approved by the Ethics Committee of the Faculty of Medicine of Masaryk University (n. 47499/2013-8) and performed in accordance with the international ARRIVE guidelines.²⁹ Localized tumors were established in immunodeficient NOD-*scid* IL2Ry^{null} mice strain³⁰ (Charles River Laboratories, Cologne, Germany) using a subcutaneous injection of MEC-1 cell line (5×10⁶ cells per animal). Mice were matched according to initial tumor size and randomized to treatment with MU380 in 20% aqueous Kolliphor solution (single inhibitor dose 20 mg/kg) or 20% Kolliphor alone. Additional information is included in the *Online Supplementary Appendix*.

Statistical analyses

Significance level was set as: **P*<0.05; ***P*<0.01; ****P*<0.001; = : not significant. The standard level of statistical significance was

$P < 0.05$. Detailed information is available in the *Online Supplementary Appendix*.

Results

Enantioselective synthesis of MU380

In order to prepare sufficient quantities of MU380 for *in vivo* studies, we developed its enantioselective synthesis from commercially available *N*-Boc-(*R*)-nipecotic acid **1** (Figure 1). Briefly, acid **1** was converted into the Weinreb amide **2**, whose treatment with deprotonated acetonitrile at low temperature afforded the required β -ketonitrile **3** with high optical purity [99% ee, determined by high performance liquid chromatography (HPLC) on chiral stationary phase]. Subsequent cyclization of **3** with 3-aminopyrazole proved to be quite challenging when, under a variety of reaction conditions including alcoholic solvents used in analogous synthesis of the CHK1 inhibitor SCH900776,³¹ we observed significant loss of stereochemical integrity. Finally, we found neat acetic acid to be the optimal solvent: cyclization was rapid and provided the desired pyrazolo[1,5-*a*]pyrimidine intermediate

4 in high yield (95%) and optical purity (96% ee). Using part of the sequence we had previously reported,²⁶ compound **4** was converted into advanced intermediate **11**, utilizing the in-house prepared boronate **9**. Optical purity of **11** (96% ee) was again determined by HPLC on chiral stationary phase, confirming that no loss of stereochemical integrity was associated with the post-cyclization steps of the sequence. Subsequent Boc-protection followed by regioselective bromination and deprotection provided the target compound MU380 (overall yield 33% over 10 steps). Final recrystallization from acetonitrile afforded optically pure MU380 (> 99% ee) on gram scale. For detailed procedure see the *Online Supplementary Appendix*.

MU380 effectively inhibits CHK1 kinase and sensitizes lymphoid tumor cells to gemcitabine

Our novel inhibitor showed satisfactory target-specific effects in a pilot study using cell lines established from solid tumors.²⁶ Herein, we first explored whether MU380 also efficiently inhibits CHK1 in lymphoid tumor cells. We treated NALM-6 and MEC-1 cell lines with gemcitabine, a potent inducer of RS, and analyzed impact of

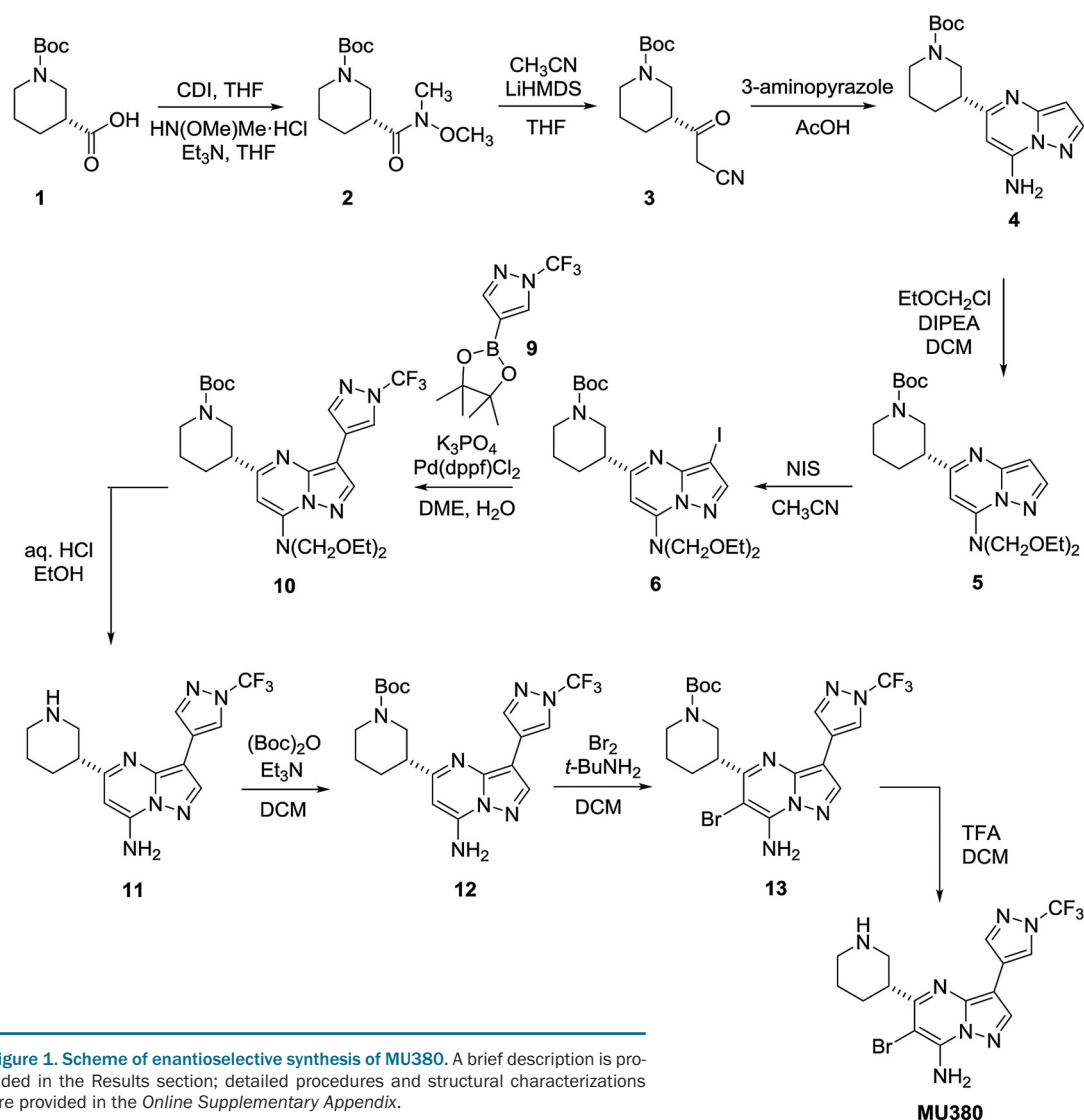


Figure 1. Scheme of enantioselective synthesis of MU380. A brief description is provided in the Results section; detailed procedures and structural characterizations are provided in the *Online Supplementary Appendix*.

the inhibitor on CHK1 protein. MU380 effectively blocked CHK1 activation (autophosphorylation pS296), while at the same time enhancing signaling from (presumably) ATR kinase towards the CHK1 (pS317 and pS345) reflecting RS potentiation (Figure 2A). MU380 also impacted the CHK1 downstream activity, which was demonstrated by reduced level of total CDC25A and CDC25C, one pS216 CDC25C isoform, pY15 CDK1, cyclin B1, and cyclin E1 (Figure 2B). The effect was more pronounced when MU380 was combined with gemcitabine.

Since effective CHK1 inhibitors should sensitize cancer cells to RS inductors, we tested the potential of MU380 in combination with gemcitabine using 10 cell lines harboring *TP53* gene disruption and 7 *TP53*-wt cell lines. MU380 (100 nM) significantly potentiated gemcitabine's efficacy in all tested cell lines (median half-maximal inhibitory concentration (IC_{50}) = 20.5 nM for gemcitabine vs. 6.5 nM for gemcitabine + MU380) (Table 1, Figure 2C, *Online*

Supplementary Table S1 and *Online Supplementary Figure S2*). As expected, MU380 enhanced the chemotherapy-induced DNA damage level, as evidenced by pS139 H2AX (γ H2AX) accumulation (Figure 2D). Altogether, MU380 effectively inhibited CHK1 in lymphoid cancer cells.

MU380 manifests single-agent activity in both p53-wt and p53-mutated cell lines

Certain cancer cell lines including those of hematopoietic origin have been shown to be sensitive to single-agent CHK1 inhibition.^{20,32} Along these lines, we tested MU380 alone in 10 leukemia and 9 lymphoma cell lines; an additional four non-cancerous cell cultures were also tested. The cancer cell lines responded with concentration-dependent viability decrease, which was similar in the *TP53*-wt (n=8) and *TP53*-mutated (n=11) samples (median IC_{50} = 330 and 392 nM, respectively) (Table 1 and Figure 3A). Interestingly, leukemia cell lines were significantly more sensitive than lymphoma lines (median IC_{50} = 238 and 401

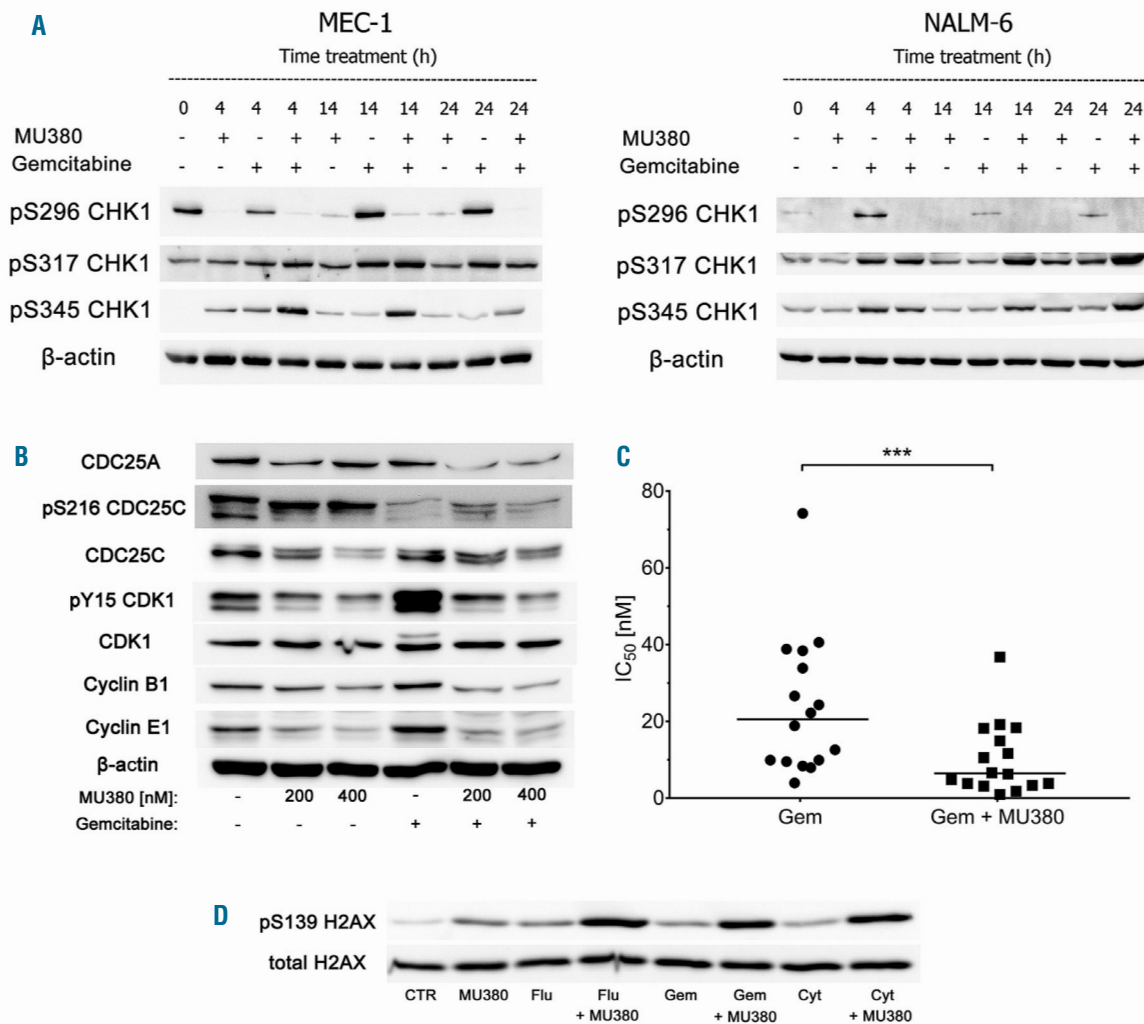


Figure 2. MU380 is effective in lymphoid tumor cells. (A) Effects on the phosphorylation status of CHK1. The cells were treated for the indicated time with MU380 (200 nM), gemcitabine (MEC-1 cell line: 10 ng/mL; NALM-6 cell line: 5 ng/mL) or combination of the agents. (B) Blocking of CHK1 downstream targets after 24 hours (h) treatment with MU380. Gemcitabine: 10 ng/mL. (C) Synergy with gemcitabine. The combined treatment of MU380 (100 nM) with gemcitabine affected viability (measured by WST-1) of the cell lines significantly more than gemcitabine alone ($P < 0.001$). Note: the graph does not involve the JEK0-1 cell line, in which IC_{50} for gemcitabine alone was not reached. $***P < 0.001$. (D) MU380 (200 nM; 24 h) potentiates DNA damage in MEC-1 cells treated with nucleoside analogs. Fludarabine (Flu): 5 μ g/mL; gemcitabine (Gem): 5 ng/mL; cytarabine (Cyt): 100 ng/mL; CTR: untreated control.

nM, respectively) (Figure 3B). Four cell lines were tested within the project of DepMap and lethal phenotype with the CHEK1 elimination using CRISPR was noted (*Online Supplementary Figure S4*). Although some cell lines manifested a high baseline RS level (see phosphorylated CHK1 isoforms and/or γ H2AX in *Online Supplementary Figure S3A*), we did not observe an apparent correlation to the viability decrease (*Online Supplementary Figure S3B*).

Essentially, non-cancerous cells were much less sensitive to MU380, specifically: immortalized epithelial cells (RPE-1 cell line) ($IC_{50} > 10 \mu M$), immortalized bone

marrow/stromal fibroblasts (HS-5 cell line) ($IC_{50} = 3.7 \mu M$), primary skin fibroblasts ($IC_{50} = 3.7 \mu M$), and primary skin fibroblasts from a patient with ataxia telangiectasia harboring complete *ATM* gene inactivation ($IC_{50} > 10 \mu M$) (*Online Supplementary Figure S3*).

To elucidate MU380 mechanistic effects, we analyzed cell cycle profile and apoptosis in six selected cell lines. The inhibitor (400 nM, 24 h treatment) significantly affected the cell cycle profile in CLL-derived cell lines: *TP53*-mutated MEC-1 and MEC-2 exhibited profound S-phase accumulation together with G_2/M phase decrease, while

Table 1. Effects of MU380 in cancer cell lines and non-cancerous cells.

Cell lines / Cells	Cancer	<i>TP53</i> status	Other genetics	Synergy with Gem	Single-agent MU380 (IC_{50} ; μM)
MEC-1	CLL/PL	c.949dupC p.Q317fs	NA	+++	0.20
MEC-2	CLL/PL	c.949dupC p.Q317fs	NA	+++	0.41
BL-41	BL	c.743G>A p.R248Q	t(8;14) (<i>MYC/IGH</i>)	+++	0.38
SU-DHL-4	DLBCL	c.817C>T p.R273C	t(14;18) (<i>IGH/BCL2</i>)	+++++	0.40
JEKO-1	MCL	c.173delC p.P58X	t(11;14) (<i>CCND1/IGH</i>)	++++	0.39
NALM-16	ALL	c.868_869insTC p.R290fs	NA	++++	0.20
RAJI	BL	c.638G>A; p.R213Q c.700T>C; p.Y234H	t(8;14) (<i>MYC/IGH</i>)	+++	0.50
REC-1	MCL	c.734G>A; p.G245D c.949C>T; p.Q317X	t(11;14) (<i>CCND1/IGH</i>)	+++	0.48
REH	ALL	c.541C>T p.R181C	t(12;21) (<i>TEL/AML1</i>)	ND	0.25
MAVER-1	MCL	c.843C>G p.D281E	t(11;14) (<i>CCND1/IGH</i>)	++++	0.25
MINO	MCL	c.440T>G p.V147G	t(11;14) (<i>CCND1/IGH</i>)	+++	0.46
OSU-CLL	CLL	WT	NA	+++	0.22
JVM-2	B-PLL	WT	t(11;14) (<i>CCND1/IGH</i>)	+++	0.22
JVM-3	B-PLL	WT	NA	+++	0.34
WSU-NHL	DLBCL	WT	t(14;18) (<i>IGH/BCL2</i>)	++++	0.32
DOHH-2	FL	WT	t(8;14;18) (<i>MYC/IGH/BCL2</i>)	+++	0.43
NALM-6	ALL	WT	t(5;12) (<i>ETV6/PDGFRB</i>)	+++	0.38
GRANTA-519	MCL	WT (del 17p)	t(11;14) (<i>CCND1/IGH</i>)	+++	ND
OCI-AML3	AML	WT	NA	ND	0.34
MOLM-13	AML	WT	(<i>MLL/AF9</i>)	ND	0.14
RPE-1	Non-cancerous	NA	NA	ND	>10
HS-5	Non-cancerous	NA	NA	ND	3.7
Fibroblasts normal	Non-cancerous	NA	NA	ND	3.7
Fibroblasts AT	Non-cancerous	NA	NA	ND	>10

Genetic characteristics of the cell lines were adopted from the German Collection of Microorganisms and Cell Cultures (DSMZ). Statistical evaluation of the synergy between MU380 and gemcitabine (Gem) was done by Chou-Talalay test; +++++ very strong synergism; ++++ strong synergism; +++ synergism; NA: not applicable; ND: not determined. CLL/PL: chronic lymphocytic leukemia in prolymphocytoid transformation; BL: Burkitt lymphoma; DLBCL: diffuse large B-cell lymphoma; MCL: mantle cell lymphoma; ALL: acute lymphoblastic leukemia; B-PLL: B-cell prolymphocytic leukemia; FL: follicular lymphoma; AML: acute myeloid leukemia. Characterization of the non-cancerous cells and cell lines is provided in *Online Supplementary Appendix*.

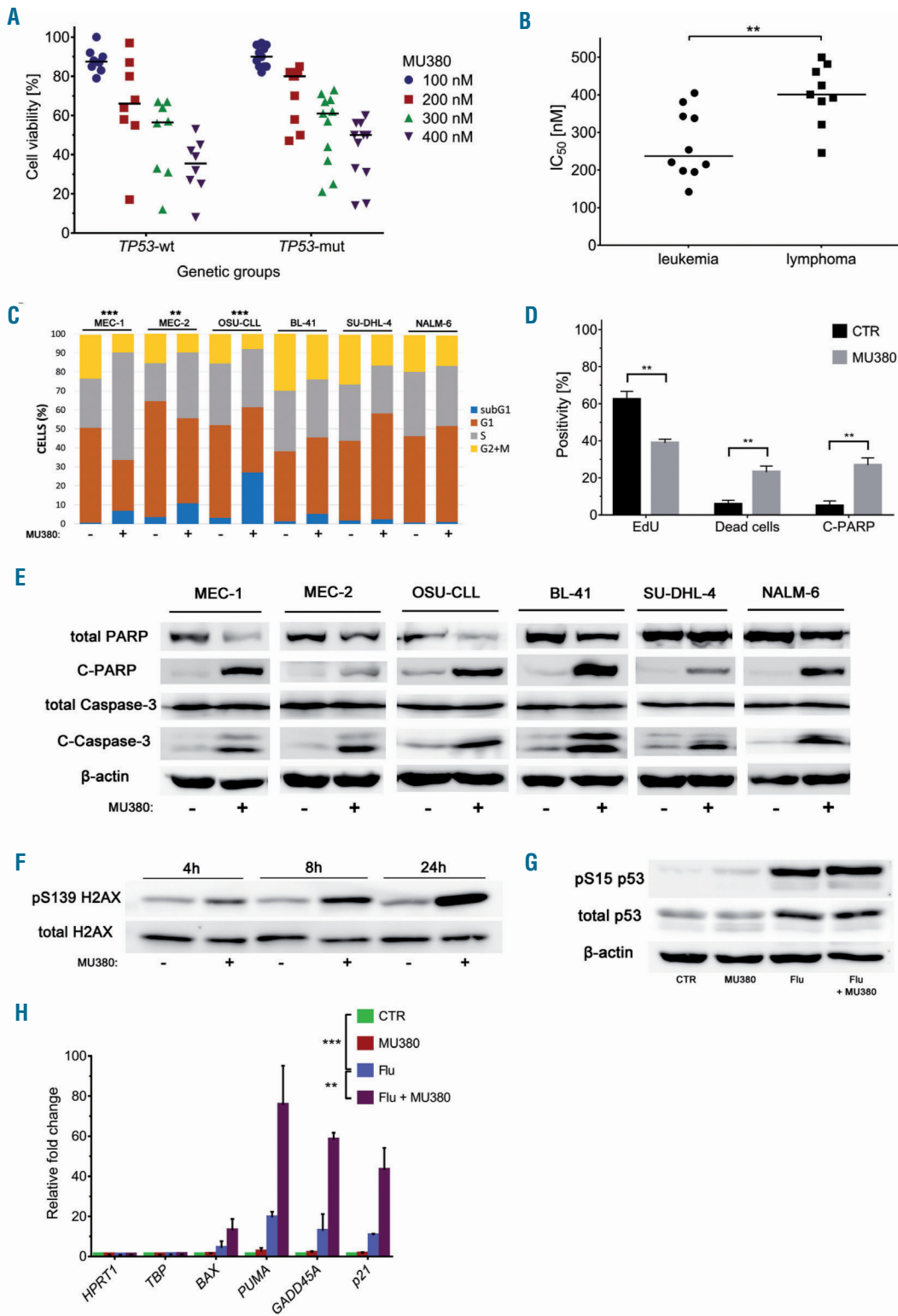


Figure 3. Effects of MU380 (single-agent) on leukemia and lymphoma cell lines. (A) Cell viability was reduced similarly in the *TP53*-wt and *TP53*-mutated cell lines ($P=0.257$) after 72 hours (h) treatment. (B) Distribution of IC_{50} values in leukemia and lymphoma cell lines ($P=0.004$). (C) MU380 (400 nM; 24 h) significantly changed the cell cycle profile in MEC-1 ($P<0.001$), MEC-2 ($P=0.010$) and OSU-CLL ($P<0.001$) cell lines; the other three cell lines showed insignificant differences. (D) MEC-1 cells treated with MU380 (400 nM; 24 h) exhibited significantly reduced DNA synthesis rate compared to control untreated cells (lower EdU incorporation, $P=0.001$) and consequently manifested extensive apoptosis as evidenced by the PARP protein cleavage ($P=0.001$). The cell death was also confirmed using labeling with Live/Dead Red agent ($P=0.002$). Graph summarizes results of three independent experiments. (E) MU380 (400 nM; 48 h) elicited apoptosis in all tested cell lines as evidenced through the cleaved PARP (C-PARP) and caspase-3 (C-Caspase-3) proteins. Note: the cell lines were exposed individually on UVITEC detection instrument; hence, intensity of the bands among the cell lines cannot be mutually compared. (F) The time-dependent γ H2AX accumulation reflects gradually increasing RS after treatment with MU380 (400 nM); the cells were harvested at indicated time points. (G) MU380 (400 nM; 24 h) does not change the p53 protein level in p53-wt NALM-6 cell line, in contrast to fludarabine (2.7 μ M; positive control). (H) MU380 (400 nM; 24 h) induces negligible expression of p53 target genes *BAX*, *PUMA*, *GADD45A*, and *CDKN1A* (p21), in contrast to fludarabine (2.7 μ M; positive control). The fold change is related to the untreated control (CTR). The graph summarizes results of two independent real-time polymerase chain reaction analyses. Error bars represent standard deviation. ** $P<0.01$; *** $P<0.001$.

TP53-wt OSU-CLL cells manifested extensive sub-G1 peak (Figure 3C and *Online Supplementary Figure S5*). In MEC-1 cells, we also recorded greatly reduced DNA synthesis rate and concurrently apparent apoptosis induction (cleavage of PARP protein) after MU380 treatment (Figure 3D and *Online Supplementary Figure S6*). Apoptosis was also detected in all other tested cell lines using western blot analysis of cleaved PARP and Caspase-3 proteins (Figure 3E). In contrast, no significant apoptosis induction was observable in non-cancerous human cell lines and primary fibroblasts (*Online Supplementary Figure S7*). Cell death was likely a consequence of enhanced DNA damage as evidenced by γ H2AX accumulation in MU380-treated cells (Figure 3F).

All aforementioned results indicate that MU380 activity is not dependent on p53 status, which is further supported by absence of p53 protein accumulation after treating the p53-wt NALM-6 cell line with MU380 (Figure 3G), as well as by negligible induction of p53-downstream target genes *CDKN1A* (*p21*), *PUMA*, *BAX*, and *GADD45* in this cell line; interestingly, the inhibitor further increased the expression elicited by fludarabine (Figure 3H).

MU380-mediated CHK1 inhibition affects transition of MEC-1 cells into mitosis

CHK1 protein inhibition abrogates the intra-S and G2/M cell cycle checkpoints.^{33,34} In p53-deficient cells lacking a functional G1/S checkpoint, CHK1 suppression can result in premature mitosis involving unrepaired DNA damage.³⁴ We hence employed a *TP53*-mutated MEC-1 cell line, in which MU380 significantly affected the cell cycle profile, and analyzed mitoses, specifically mitotic index (MI) and integrity of mitotic chromosomes. In addition to CHK1 inhibition, we also examined parallel blocking of ATR to assess contribution of this closely co-operating kinase to the studied phenotypes; in a recent study, ATR/CHK1 co-inhibition exhibited a surprising synergy in cancer cells, which was attributed to accentuated replication collapse.³⁵ For ATR depletion, we used selective inhibitor VE-821,³⁵ which blocked ATR-mediated CHK1 phosphorylations (pS317/pS345) in MEC-1 cells (*Online Supplementary Figure S8*).

The results of two independent experiments are summarized in Table 2. After treatment with MU380 alone,

Table 2. Cytogenetic analysis in MEC-1 cell line.

Experiment 1	Mitotic index (%)	Analyzed mitoses	Cells with breaks
Control	11.5	50	0
CHK1i	3.0	50	7
ATRi	10.8	50	7
CHK1i + ATRi	5.7	50	19

Experiment 2	Mitotic index (%)	Analyzed mitoses	Cells with breaks
Control	18.0	50	0
CHK1i	2.2	54	4
ATRi	18.5	55	19
CHK1i + ATRi	3.9	52	27

The cells were treated for 24 hours with the following agents: Experiment 1: 200 nM MU380 (CHK1i); 1 μ M VE-821 (ATRi); respective combination. Experiment 2: 400 nM MU380, 2 μ M VE-821; respective combination.

the MI sharply decreased, and a proportion of mitotic cells manifested chromosome damage in some cells resembling pulverization (*Online Supplementary Figure S9*). Remarkably, with cells co-treated by CHK1 and ATR inhibitors we measured a higher MI compared to the CHK1 inhibitor alone. In line with this observation, we also recorded a higher proportion of cells with chromosome damage.

MU380 induces cell death in dividing and non-dividing primary chronic lymphocytic leukemia lymphocytes

We subsequently tested MU380 single-agent activity in primary CLL cells using vitally frozen clinical samples. Since CLL lymphocytes obtained from patient peripheral blood manifest only weak ATR/CHK1 pathway activity,^{23,36} we initially stimulated proliferation of CLL cells using the anti-CD40/IL-4 system.^{24,28} This stimulation shifted a significant part of the CLL cells to post-G1 phases of the cell cycle, which was apparent from both the DNA content analysis and enhanced expression of proliferation markers, *MKI67* and *BIRC5* (coding survivin) (*Online Supplementary Figure S10*). The stimulation also results in upregulation of activated CHK1 protein as we previously reported²⁴ and in enhanced anti-apoptotic signaling.³⁷

In the stimulated CLL cells, MU380 effectively elicited RS (pS345 CHK1) and abrogated CHK1 activation (pS296) (Figure 4A). The impact on cell viability was tested in 13 stimulated CLL cultures harboring adverse genetic features including *TP53* mutations, *ATM* mutations, and/or complex karyotype (*Online Supplementary Table S2*). Notably, MU380 reduced viability of these samples with different genetic background to a similar extent; the IC_{50} value was approximately 1 μ M in all but one sample (Figure 4B). Cell death mechanism included apoptosis as evidenced by the PARP protein cleavage (Figure 4C).

Consequently, we investigated non-stimulated primary CLL cells, which manifest a low but detectable CHK1 protein level (Figure 5A). Historically, the ATR pathway was considered to be inactive in quiescent lymphocytes,³⁸ such as those from CLL patients. However, a recent study³⁶ reported that ATR is active in primary CLL cells, and accordingly we detected a rise in pS345 CHK1 level after treatment with fludarabine (Figure 5B). We also confirmed that MU380 leads to blockade of CHK1 autophosphorylation at S296 (Figure 5C). Moreover, we noticed reduction of the CDC25C protein level; however, it was not detectable in all tested samples (*Online Supplementary Figure S11*).

To address MU380 impact on cell viability, we tested 96 non-stimulated CLL cultures (*Online Supplementary Table S3*). A vast majority of these non-dividing CLL cells responded to the inhibitor (100-400 nM) by clear concentration-dependent viability decrease, with insignificant differences among studied genetic groups: *TP53*-mutated samples, mean IC_{50} = 337 nM; *ATM*-mutated samples 385 nM; 11q- deleted samples (the other *ATM* allele intact) 355 nM; and *ATM*-wt/*TP53*-wt samples 414 nM; healthy PBMNC cultures were virtually inert to MU380 (Figure 5D). Apoptosis induction was already apparent at 100 nM MU380 (Figure 5E). We also recorded similar response when our CLL cultures were clustered according to the presence of *SF3B1* mutations, *NOTCH1* mutations, *IGHV* status, complex karyotype presence, or their therapy status (*Online Supplementary Figure S12*).

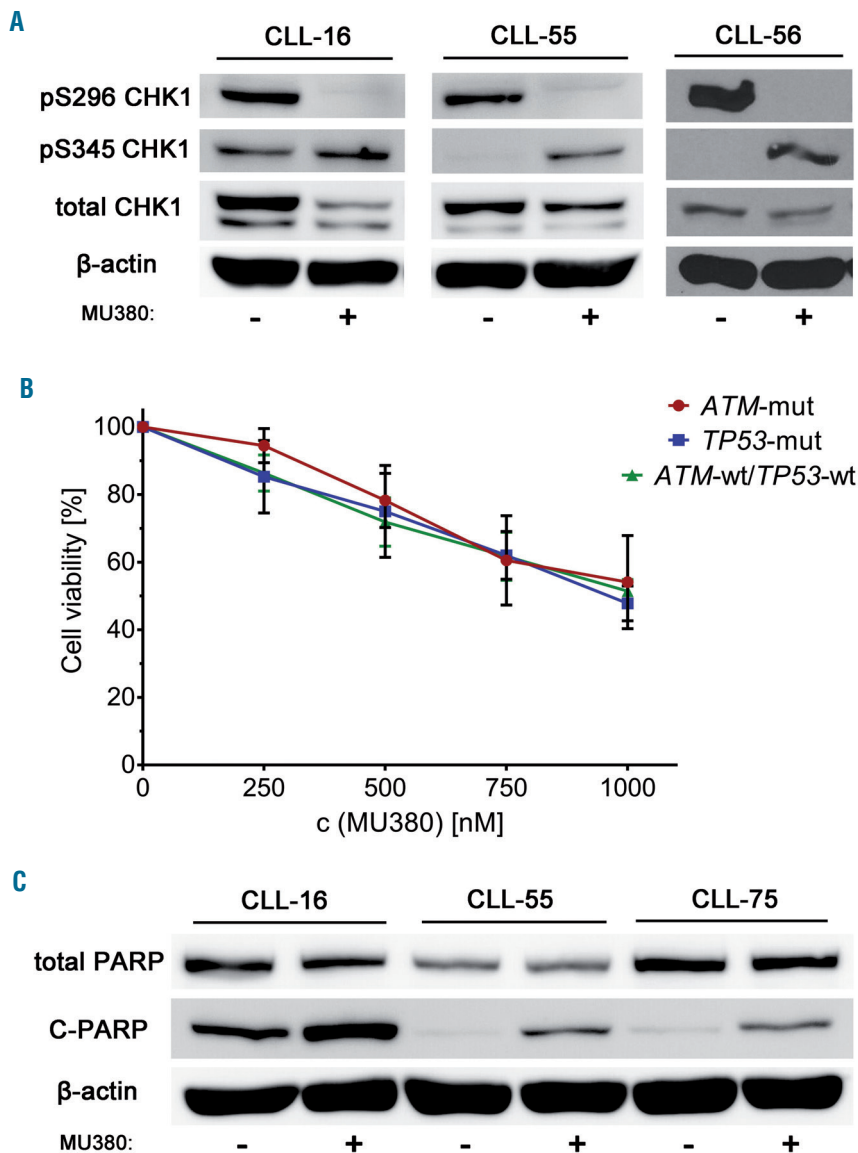


Figure 4. Effects of MU380 in chronic lymphocytic leukemia (CLL) cells pre-treated with pro-proliferative stimuli. Primary CLL cells were cultured in the presence of pro-proliferative stimuli for ten days and subsequently treated with MU380. (A) MU380 [1 μ M; 24 hours (h)] enhanced RS (pS345) and abrogated CHK1 protein activation (pS296). (B) The 72-h treatment with MU380 reduced viability of all tested samples; *TP53*-mutated (n=7), *ATM*-mutated (n=3) and *TP53*-wt/*ATM*-wt (n=3). The effect was similar (IC_{50} approx. 1 μ M) with the exception of sample CLL-75 harboring complete *ATM* inactivation (viability 66% at 1 μ M MU380). Error bars represent standard deviation. (C) The 48 h treatment with 1 μ M MU380 led to cleavage of PARP protein (C-PARP) in the tested samples.

Importantly, we also confirmed a decrease in viability in CLL cells after transfection with siRNA targeting CHEK1 (Figure 5F and *Online Supplementary Figure S13*). Moreover, to rule out the possibility of compound-specific MU380 effects, we confirmed a decrease in viability in non-stimulated CLL cells using structurally different CHK1 inhibitor CHIR-124³⁹ (*Online Supplementary Figure S14*). The mechanism of cell death caused by MU380 treatment included apoptosis (PARP protein cleavage was detected in 19 of 22 tested samples), which was probably a consequence of DNA damage accumulation (γ H2AX rise in 8 of 10 samples). Concerning MU380 impact on apoptosis-associated proteins, we noted a frequent decrease in MCL1 (7 of 9 samples) and NF- κ B (7 of 12 samples), whilst there was no change in the level of BCL2 (12 samples tested). MU380 also reduced the MYC protein level in 4 of 6 samples and total CHK1 level in 17 of 23 samples. Western blots for all proteins listed above are presented in *Online Supplementary Figure S15*.

Similarly to cell lines, we observed no accumulation of p53 protein or its downstream target genes after treatment of primary (p53-wt) CLL samples with MU380; in contrast, inhibitor did not further increase the expression elicited by fludarabine (Figure 5G and H).

MU380 suppresses growth of TP53-mutated subcutaneous tumors *in vivo*

Finally, we also tested the activity of MU380 *in vivo* using immunodeficient mice strain NOD-*scid* IL2R γ^{null} with subcutaneous tumors generated from MEC-1 cells similarly as reported by Attianese *et al.*⁴⁰ In line with our previous study,⁴¹ subcutaneous tumors were readily visible on day +14 post transplant; the tumors consisted of proliferating MEC-1 cells (Ki-67- and CD20-positive) (Figure 6A). In experiment I, we administered seven doses of MU380 between days +14 and +28 post transplant, and the sequential measurement of tumor volume revealed significantly suppressed growth in the inhibitor group (n = 7

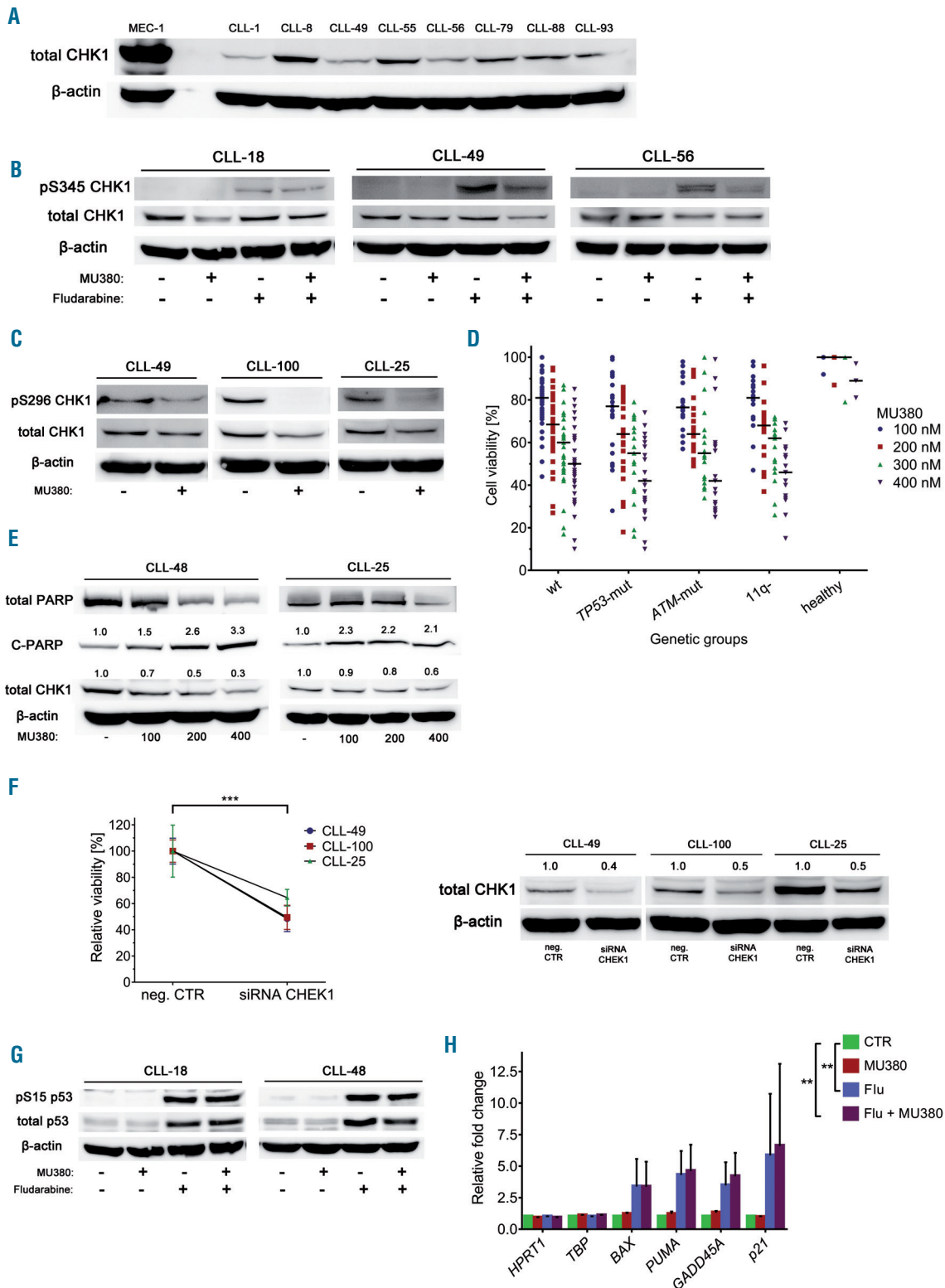


Figure 5. CHK1 protein level and effects of MU380 in non-stimulated chronic lymphocytic leukemia (CLL) cells. (A) The CHK1 protein was detectable in all tested CLL samples using the sensitive detection kit. (B) The treatment with fludarabine [10 μM; 24 hours (h)] resulted in phosphorylation of the CHK1 protein on Ser345 residue indicating its activation. (C) Reduction of pS296 autophosphorylation after MU380 treatment (400 nM, 24 h). (D) The 72 h treatment with MU380 (100-400 nM) decreased viability of most CLL samples, with insignificant differences among the studied samples; wt-ATM/wt-TP53 (wt) versus TP53-mut $P=0.199$; versus ATM-mut $P=0.964$; versus 11q- (the other ATM allele intact) $P=0.849$. The healthy peripheral blood mononuclear cell samples ($n=3$) were substantially less affected ($P<0.001$). (E) MU380 elicited apoptosis as evidenced by the cleaved PARP (C-PARP) protein. The values indicate densitometric analysis set to 1.0 in control. (F, left) Viability decrease in CLL cells transfected with siRNA targeting CHEK1. (F, right) Decrease in the CHK1 protein level after transfection with siRNA targeting CHEK1. (G) MU380 (400 nM; 24 h) did not change the p53 protein level in TP53-wt samples, in contrast to fludarabine (10 μM; positive control). (H) MU380 (400 nM; 24 h) did not induce expression of p53-downstream target genes BAX, PUMA, GADD45A, and CDKN1A (p21), in contrast to fludarabine (10 μM; positive control). The fold change is related to untreated control (CTR). The graph summarizes results of real-time polymerase chain reaction analyses in three samples (CLL-58, CLL-77, CLL-83). Error bars represent standard deviation. *** $P<0.001$; ** $P<0.01$.

mice) compared to control animals (n = 8 mice) on average by approximately 44% (Figure 6B and C). In experiment II, we administered ten doses of MU380 between days +14 and +25 post-transplant (inhibitor group n = 15 mice; control group n = 8 mice), which again resulted in pronounced tumor growth suppression on average by ~ 61% in this case (Figure 6D).

The tumor cells from mice treated with MU380 exhibited a significantly increased RS level as evidenced by accumulation of γ H2AX (Figure 6E and F) and pS345 CHK1 (Figure 6F), while also manifesting moderately increased apoptosis (Figure 6E).

No apparent adverse effects were observed in either experiment.

Discussion

Chronic lymphocytic leukemia has long been considered a disease caused by gradual accumulation of malignant B lymphocytes with disabled apoptosis induction. However, this static view changed dramatically when Messmer *et al.*⁴² reported data on CLL cell kinetics *in vivo*, revealing that malignant cell turnover is much higher than appreciated, and may reach over 1% of a total clone per day. Lymph nodes are the primary site of CLL cell proliferation *in vivo*;^{43,44} approximately one-fourth of leukemic cells in this compartment possess proliferative potential.⁴⁵ Beside a simple cell renewal, proliferation is a prerequisite for clonal selection of new genetic variants, and this phenomenon is currently well-documented in CLL.⁴⁶ Furthermore, CLL genome is characterized by deregulated expression of genes involved in DNA replication, repair and recombination.⁴⁷ Taking these observations into account, we surmised that targeting dividing leukemic cells may represent a therapeutic strategy in CLL and therefore hypothesized that CHK1 kinase, which is essential for DNA replication and recombination-based repair, can be a suitable target.

We initially focused on obtaining sufficient quantities of the metabolically robust CHK1 inhibitor MU380. Although structurally related clinical candidate SCH900776 can certainly be considered one of the most specific CHK1 inhibitors with excellent selectivity for CHK1 over CHK2 or cyclin-dependent kinases,^{24,25} its metabolic profile may not be optimal. Specifically, SCH900776 contains the N-methylpyrazole motif, which undergoes oxidative demethylation resulting in the formation of significantly less selective metabolite and a rapid decrease of active concentration in plasma.²⁶ In contrast, MU380 contains highly unusual N-trifluoromethylpyrazole pharmacophore, which provides substantially better metabolic robustness and pharmacokinetic profile.²⁶

The newly developed enantioselective synthesis of MU380 described here provides access to gram quantities of enantiomerically pure substance, which enables thorough *in vivo* testing of the compound.

In our *in vivo* experiments with xenotransplanted MEC-1 cells, MU380 elicited strong and reproducible tumor growth suppression that was accompanied by an adequate molecular phenotype, namely the RS accumulation. Although the induction of apoptosis was rather modest, encouraging *in vivo* activity of MU380 opens up further opportunities to test more intense administration of the

compound and/or its combination with additional appropriate agents.

MU380 exhibited interesting single-agent activity in tested leukemia and lymphoma cell lines that responded *via* viability decrease with IC₅₀ values between 142 and 500 nM. By virtue of this relatively uniform good reaction, we were not able to find determinants that would further stratify the response, except that leukemia cell lines were more sensitive than lymphoma ones. Although we hypothesized that a distinct RS level could justify this observation, baseline CHK1 phosphorylations and γ H2AX, standard markers of RS, did not correlate with the leukemia/lymphoma status.

Throughout our study, we focused on MU380 effects in TP53-mutated lymphoid cells. Hypothetically, CHK1 inhibition should be effective in a p53-deficient background due to dysfunction of all major cell cycle checkpoints and consequently complete impairment of cell cycle control potentially resulting in mitotic catastrophe. Nevertheless, our study indicates that this concept of “inducing death by releasing the breaks”⁷⁵⁴ may not be completely straightforward. Initially, certain p53 mutated cells surprisingly manifest G1-phase accumulation upon CHK1 inhibition, which we consistently observed, for example, in SU-DHL-4 cell line. Moreover, even the cells responding to CHK1 inhibition by more forthcoming S-phase accumulation and G2/M phase decrease are probably equipped with relevant mitotic entry control. This was apparent from the co-inhibition of ATR with CHK1, which resulted in increased MI and chromosome damage compared to the sole CHK1 inhibition. In this respect, recently recorded synergy between CHK1 and ATR inhibition may not only be a consequence of more pronounced replication collapse,³⁵ but of increased mitotic damage as well.

Beside the proliferative fraction, the CLL cell population also consists of non-dividing cells arrested either at the G₀ (quiescent cells) or G₁ phase of the cell cycle.⁴⁵ Intuitively, such cells might not respond to CHK1 inhibition due to low ATR^{23,38} and CHK1 levels.^{11,48} Nevertheless, a recent study⁴⁹ reported apoptosis induction in non-dividing CLL cells caused by treatment with a dual CHK1/CHK2 inhibitor AZD7762. Moreover, we found that *CHEK1* is targetable in CLL cells using siRNA transfection. Another recent work by Beyaert *et al.*³⁶ concluded that ATR, despite its low level, is active in quiescent CLL cells and phosphorylates downstream targets upon DNA damage induction. Here, to our knowledge for the first time, we document that non-stimulated CLL cells also phosphorylate CHK1 upon DNA damage, despite the fact that their CHK1 level is low. Notably, we also observed significant MU380 single-agent activity in non-dividing CLL cells. Although the set of samples was enriched by those with therapeutically unfavorable genetics, only a few were resistant to our inhibitor. In fact, only 5 of 96 samples showed viability \geq 80% after 72 h treatment. Interestingly, 3 of 5 samples harbored complete *ATM* inactivation (2 others were *ATM*-wt/*TP53*-wt). Thus, although the *ATM*-mutated samples on average did not manifest resistance, some of them were particularly refractory. It is intriguing that non-cancerous cells with *ATM* inactivation (fibroblasts from *ataxia-telangiectasia* patient) also manifested strong resistance to MU380.

Overall, our results support the concept that CHK1 is a critical protein for B-cell lymphomagenesis and that even

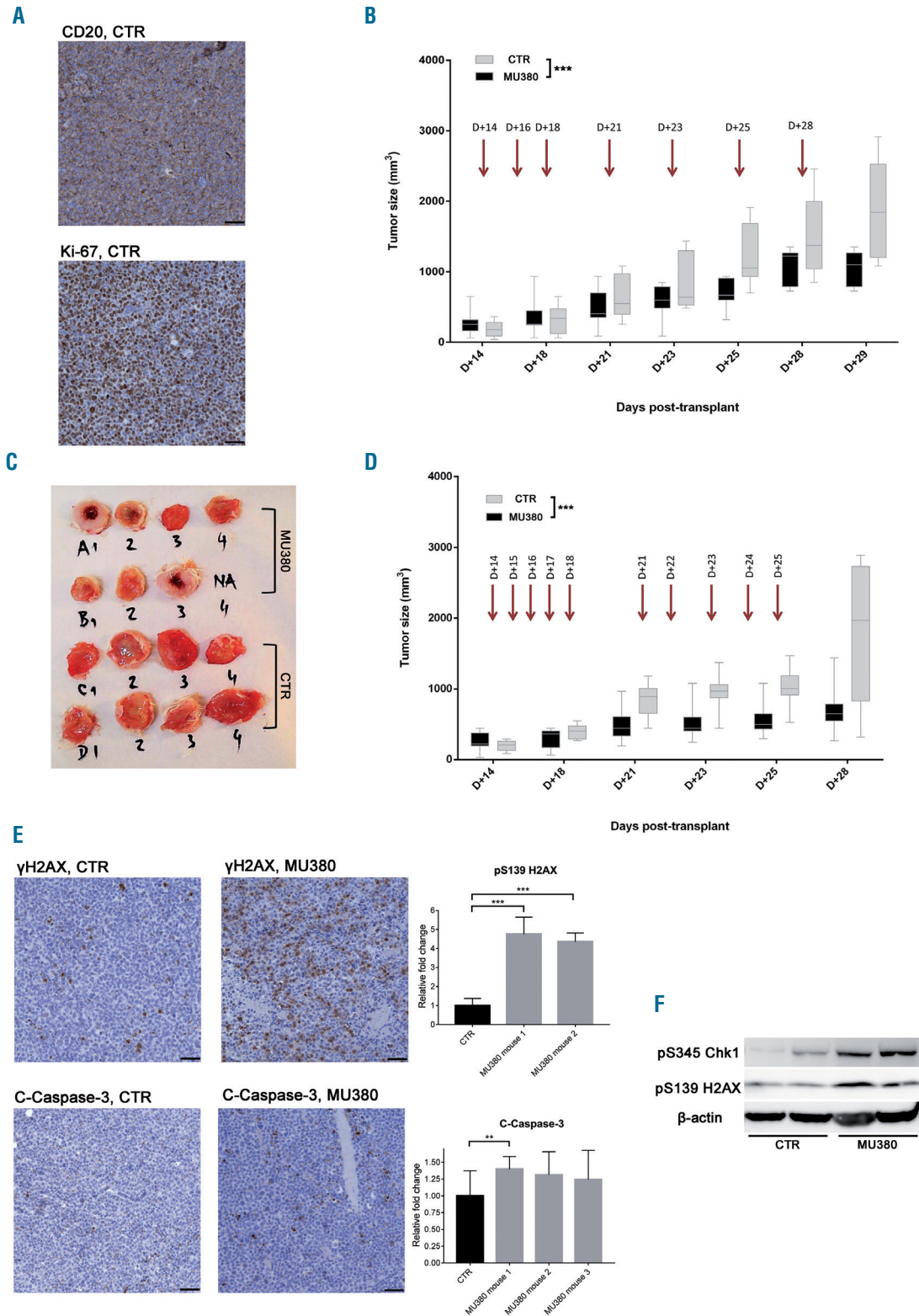


Figure 6. MU380 suppresses tumor growth *in vivo*. (A) Immunohistochemical analysis of tumors. The tumors consisted dominantly of MEC-1 cells expressing the B-cell specific antigen CD20. The cells were proliferating showing the high Ki-67 positivity. Bars represent 50 μ m. (B) Growth of the tumors in experiment I. Mean tumor volume at day (D)+29 was 1897 mm³ in the control group (CTR) and 1072 mm³ in the inhibitor group ($P < 0.001$). Arrows mark the administration of MU380 (20 mg/kg) or 20% aqueous Kolliphor alone (mock control). (C) The tumors extracted at D+29 post transplant in Experiment I. MU380: tumors from mice treated with the inhibitor; CTR: tumors from control mice. (D) Growth of the tumors in experiment II. Mean tumor volume at D+28 was 1771 mm³ in the control group and 695 mm³ in the inhibitor group ($P < 0.001$). Arrows mark the administration of MU380 (20 mg/kg) or 20% aqueous Kolliphor alone (mock control). (E, top left) The replication stress was significantly increased in tumor cells from mice treated with MU380 compared to those from control animals (CTR) ($P < 0.001$). (E, bottom left) In the same comparison, apoptosis increase was modest. Samples were collected 24 h after the last administration of MU380. Bars represent 50 μ m. (E, right) Quantitative evaluation of the immunohistochemical analysis. (F) Western blot analysis of replication stress markers in tumors from control and treated mice. Samples were collected 24 h after the last administration of MU380. Tumors from two control (CTR) and two treated (MU380) mice are shown. Error bars represent standard deviation. *** $P < 0.001$; ** $P < 0.01$.

resting B cells are vulnerable to CHK1 depletion.²²

The MU380 single-agent activity is noteworthy, especially in the light of the fact that CLL is typically resistant to therapy based on a single drug and that most current therapeutic regimens consist of several agents with combined mechanisms of action. In any case, it will be worthwhile analyzing potential synergy between CHK1 inhibition and current state-of-the-art CLL therapeutics targeting BCR signaling or BCL2 protein. Such analysis was not within the scope of this pilot study, but preliminary data we obtained with MEC-1 cells indicate an approximate additive effect of MU380 combined with ibrutinib (Boudny *et al.*, 2019, unpublished observation). Furthermore, a recent study focusing on molecular analysis of druggable pathways in blood cancers⁴⁹ determined that the CLL cell response to SCH900776 is distinct from that of BCR pathway inhibitors. Concerning BCL2, at least the total level of this protein is unaffected by MU380. It might, therefore, be interesting to test a combination of MU380 with BH3-mimetics, e.g. venetoclax. Since MU380 reduces important anti-apoptotic proteins MCL1 and NF- κ B activated by

BCR signaling in CLL cells,^{45,50} response to combination treatment could, indeed, be synergistic.

In summary, we have demonstrated that our novel CHK1 inhibitor MU380 effectively affects both dividing and non-dividing CLL cells harboring *TP53* mutations. Consequently, CHK1 inhibition may represent an attractive therapeutic option for high-risk CLL.

Funding

The work was supported by Grant n. 15-33999A provided by the Ministry of Health of the Czech Republic, Project FNBr 65269705 – Conceptual Development of Research Organization, Project MUNI/A/1105/2018, Project

CZ-OPENSREEN: National Infrastructure for Chemical Biology (Identification code: LM2015063), and by the National Program of Sustainability II (project No. LQ1605) and CEITEC 2020 Project (LQ1601) provided by the Ministry of Education, Youth and Sports of the Czech Republic. We thank Veronika Sandova for advice with transfection experiments and Olga Stehlikova for help with flow cytometry. We thank Richard Zimmerman for his English editing.

References

- Seda V, Mraz M. B-cell receptor signalling and its crosstalk with other pathways in normal and malignant cells. *Eur J Haematol.* 2015;94(3):193-205.
- Thompson PA, Burger JA. Bruton's tyrosine kinase inhibitors: first and second generation agents for patients with Chronic Lymphocytic Leukemia (CLL). *Expert Opin Investig Drugs.* 2018;27(1):31-42.
- Daniel C, Mato AR. BCL-2 as a therapeutic target in chronic lymphocytic leukemia. *Clin Adv Hematol Oncol.* 2017;15(3):210-218.
- Mato AR, Nabhan C, Thompson MC, et al. Toxicities and outcomes of 616 ibrutinib-treated patients in the United States: a real-world analysis. *Haematologica.* 2018;103(5):874-879.
- Maddocks KJ, Ruppert AS, Lozanski G, et al. Etiology of Ibrutinib Therapy Discontinuation and Outcomes in Patients With Chronic Lymphocytic Leukemia. *JAMA Oncol.* 2015;1(1):80-87.
- O'Brien S, Furman RR, Coutre S, et al. Single-agent ibrutinib in treatment-naïve and relapsed/refractory chronic lymphocytic leukemia: a 5-year experience. *Blood.* 2018;131(17):1910-1919.
- Jones J, Mato A, Coutre S, et al. Evaluation of 230 patients with relapsed/refractory deletion 17p chronic lymphocytic leukaemia treated with ibrutinib from 3 clinical trials. *Br J Haematol.* 2018;182(4):504-512.
- Stilgenbauer S, Schnaiter A, Paschka P, et al. Gene mutations and treatment outcome in chronic lymphocytic leukemia: results from the CLL8 trial. *Blood.* 2014;123(21):3247-3254.
- Thompson R, Eastman A. The cancer therapeutic potential of Chk1 inhibitors: how mechanistic studies impact on clinical trial design: Therapeutic potential of Chk1 inhibitors. *Br J Clin Pharmacol.* 2013;76(3):358-369.
- González Besteiro MA, Gottifredi V. The fork and the kinase: a DNA replication tale from a CHK1 perspective. *Mutat Res Rev.* 2015;763:168-180.
- Bartkova J, Horejsí Z, Koed K, et al. DNA damage response as a candidate anti-cancer barrier in early human tumorigenesis. *Nature.* 2005;434(7035):864-870.
- de Klein A, Muijtjens M, van Os R, et al. Targeted disruption of the cell-cycle checkpoint gene ATR leads to early embryonic lethality in mice. *Curr Biol.* 2000;10(8):479-482.
- Takai H, Tominaga K, Motoyama N, et al. Aberrant cell cycle checkpoint function and early embryonic death in Chk1(-/-) mice. *Genes Dev.* 2000;14(12):1439-1447.
- Bryant C, Rawlinson R, Massey AJ. Chk1 inhibition as a novel therapeutic strategy for treating triple-negative breast and ovarian cancers. *BMC Cancer.* 2014;14:570.
- Sen T, Tong P, Stewart CA, et al. CHK1 Inhibition in Small-Cell Lung Cancer Produces Single-Agent Activity in Biomarker-Defined Disease Subsets and Combination Activity with Cisplatin or Olaparib. *Cancer Res.* 2017;77(14):3870-3884.
- Manic G, Signore M, Sistigu A, et al. CHK1-targeted therapy to deplete DNA replication-stressed, p53-deficient, hyperdiploid colorectal cancer stem cells. *Gut.* 2018;67(5):903-917.
- Lowery CD, VanWye AB, Dowless M, et al. The Checkpoint Kinase 1 Inhibitor Prexasertib Induces Regression of Preclinical Models of Human Neuroblastoma. *Clin Cancer Res.* 2017;23(15):4354-4363.
- Oo ZY, Stevenson AJ, Proctor M, et al. Endogenous Replication Stress Marks Melanomas Sensitive to CHEK1 Inhibitors In Vivo. *Clin Cancer Res.* 2018;24(12):2901-2912.
- Walton MI, Eve PD, Hayes A, et al. The clinical development candidate CCT245737 is an orally active CHK1 inhibitor with preclinical activity in RAS mutant NSCLC and Eµ-MYC driven B-cell lymphoma. *Oncotarget.* 2016;7(3):2329-2342.
- Bryant C, Scriven K, Massey AJ. Inhibition of the checkpoint kinase Chk1 induces DNA damage and cell death in human Leukemia and Lymphoma cells. *Mol Cancer.* 2014;13:147.
- Iacobucci I, Di Rorà AGL, Falzaccappa MVV, et al. In vitro and in vivo single-agent efficacy of checkpoint kinase inhibition in acute lymphoblastic leukemia. *J Hematol Oncol.* 2015;8:125.
- Schuler F, Weiss JG, Lindner SE, et al. Checkpoint kinase 1 is essential for normal B cell development and lymphomagenesis. *Nat Commun.* 2017;8(1):1697.
- Kwok M, Davies N, Agathangelou A, et al. ATR inhibition induces synthetic lethality and overcomes chemoresistance in TP53- or ATM-defective chronic lymphocytic leukemia cells. *Blood.* 2016;127(5):582-595.
- Zemanova J, Hylse O, Collakova J, et al. Chk1 inhibition significantly potentiates activity of nucleoside analogs in TP53-mutated B-lymphoid cells. *Oncotarget.* 2016;7(38):62091-62106.
- Guzi TJ, Paruch K, Dwyer MP, et al. Targeting the replication checkpoint using SCH 900776, a potent and functionally selective CHK1 inhibitor identified via high content screening. *Mol Cancer Ther.* 2011;10(4):591-602.
- Samadder P, Suchánková T, Hylse O, et al. Synthesis and Profiling of a Novel Potent Selective Inhibitor of CHK1 Kinase Possessing Unusual N-trifluoromethylpyrazole Pharmacophore Resistant to Metabolic N-dealkylation. *Mol Cancer Ther.* 2017;16(9):1831-1842.
- Petitjean A, Mathe E, Kato S, et al. Impact of mutant p53 functional properties on TP53 mutation patterns and tumor phenotype: lessons from recent developments in the IARC TP53 database. *Hum Mutat.* 2007;28(6):622-629.
- Patten PEM, Chu CC, Albesiano E, et al. IGHV-unmutated and IGHV-mutated chronic lymphocytic leukemia cells produce activation-induced deaminase protein with a full range of biologic functions. *Blood.* 2012;120(24):4802-4811.

29. Kilkenny C, Browne WJ, Cuthill IC, Emerson M, Altman DG. Improving bioscience research reporting: the ARRIVE guidelines for reporting animal research. *PLoS Biol.* 2010;8(6):e1000412.
30. Shultz LD, Lyons BL, Burzenski LM, et al. Human Lymphoid and Myeloid Cell Development in NOD/LtSz-scid IL2R γ null Mice Engrafted with Mobilized Human Hemopoietic Stem Cells. *J Immunol.* 2005;174(10):6477-6489.
31. Labroli MA, Dwyer MP, Poker C, Keertikar KM, Rossman R, Guzi TJ. A convergent preparation of the CHK1 inhibitor MK-8776 (SCH 900776). *Tetrahedron Lett.* 2016;57(24):2601-2603.
32. Davies KD, Humphries MJ, Sullivan FX, et al. Single-agent inhibition of Chk1 is antiproliferative in human cancer cell lines in vitro and inhibits tumor xenograft growth in vivo. *Oncol Res.* 2011;19(7):349-363.
33. Kawabe T. G2 checkpoint abrogators as anticancer drugs. *Mol Cancer Ther.* 2004;3(4):513-519.
34. Ma CX, Janetka JW, Piwnica-Worms H. Death by releasing the breaks: CHK1 inhibitors as cancer therapeutics. *Trends Mol Med.* 2011;17(2):88-96.
35. Sanjiv K, Hagenkorf A, Calderón-Montaña JM, et al. Cancer-Specific Synthetic Lethality between ATR and CHK1 Kinase Activities. *Cell Rep.* 2016;14(2):298-309.
36. Beyaert M, Starczewska E, Pérez ACG, et al. Reevaluation of ATR signaling in primary resting chronic lymphocytic leukemia cells: evidence for pro-survival or pro-apoptotic function. *Oncotarget.* 2017;8(34):56906-56920.
37. Natoni A, Murillo LS, Kliszczak AE, et al. Mechanisms of action of a dual Cdc7/Cdk9 kinase inhibitor against quiescent and proliferating CLL cells. *Mol Cancer Ther.* 2011;10(9):1624-1634.
38. Jones GG, Reaper PM, Pettitt AR, Sherrington PD. The ATR-p53 pathway is suppressed in noncycling normal and malignant lymphocytes. *Oncogene.* 2004;23(10):1911-1921.
39. Tse AN, Rendahl KG, Sheikh T, et al. CHIR-124, a novel potent inhibitor of Chk1, potentiates the cytotoxicity of topoisomerase I poisons in vitro and in vivo. *Clin Cancer Res.* 2007;13(2 Pt 1):591-602.
40. Giordano Attianese GMP, Marin V, Hoyos V, et al. In vitro and in vivo model of a novel immunotherapy approach for chronic lymphocytic leukemia by anti-CD23 chimeric antigen receptor. *Blood.* 2011;117(18):4736-4745.
41. Verner J, Trbusek M, Chovancova J, et al. NOD/SCID IL2R γ -null mouse xenograft model of human p53-mutated chronic lymphocytic leukemia and ATM-mutated mantle cell lymphoma using permanent cell lines. *Leuk Lymphoma.* 2015;56(11):3198-3206.
42. Messmer BT, Messmer D, Allen SL, et al. In vivo measurements document the dynamic cellular kinetics of chronic lymphocytic leukemia B cells. *J Clin Invest.* 2005;115(3):755-764.
43. Herishanu Y, Pérez-Galán P, Liu D, et al. The lymph node microenvironment promotes B-cell receptor signaling, NF-kappaB activation, and tumor proliferation in chronic lymphocytic leukemia. *Blood.* 2011;117(2):563-574.
44. Herndon TM, Chen S-S, Saba NS, et al. Direct in vivo evidence for increased proliferation of CLL cells in lymph nodes compared to bone marrow and peripheral blood. *Leukemia.* 2017;31(6):1340-1347.
45. Obermann EC, Went P, Tzankov A, et al. Cell cycle phase distribution analysis in chronic lymphocytic leukaemia: a significant number of cells reside in early G1-phase. *J Clin Pathol.* 2007;60(7):794-797.
46. Landau DA, Tausch E, Taylor-Weiner AN, et al. Mutations driving CLL and their evolution in progression and relapse. *Nature.* 2015;526(7574):525-530.
47. Grgurevic S, Berquet L, Quillet-Mary A, et al. 3R gene expression in chronic lymphocytic leukemia reveals insight into disease evolution. *Blood Cancer J.* 2016;6(6):e429.
48. Kaneko YS, Watanabe N, Morisaki H, et al. Cell-cycle-dependent and ATM-independent expression of human Chk1 kinase. *Oncogene.* 1999;18(25):3673-3681.
49. Dietrich S, Oleš M, Lu J, et al. Drug-perturbation-based stratification of blood cancer. *J Clin Invest.* 2018;128(1):427-445.
50. Petlickovski A, Laurenti L, Li X, et al. Sustained signaling through the B-cell receptor induces Mcl-1 and promotes survival of chronic lymphocytic leukemia B cells. *Blood.* 2005;105(12):4820-4827.